Characteristics of titanium oxide memristor with coexistence of dopant drift and a tunnel barrier*

Tian Xiao-Bo(田晓波)† and Xu Hui(徐 晖)

Embedded System and Solid-State Engineering Technology Center, School of Electronic Science and Engineering, National University of Defense and Technology, Changsha 410073, *China*

(Received 19 October 2013; revised manuscript received 18 December 2013; published online 10 April 2014)

The recent published experimental data of titanium oxide memristor devices which are tested under the same experimental conditions exhibit the strange instability and complexity of these devices. Such undesired characteristics preclude the understanding of the device conductive processes and the memristor-based practical applications. The possibility of the coexistence of dopant drift and tunnel barrier conduction in a memristor provides preliminary explanations for the undesired characteristics. However, current research lacks detailed discussion about the coexistence case. In this paper, dopant drift and tunnel barrier-based theories are first analyzed for studying the relations between parameters and physical variables which affect characteristics of memristors, and then the influences of each parameter change on the conductive behaviors in the single and coexistence cases of the two mechanisms are simulated and discussed respectively. The simulation results provide further explanations of the complex device conduction. Theoretical methods of eliminating or reducing the coexistence of the two mechanisms are proposed, in order to increase the stability of the device conduction. This work also provides the support for optimizing the fabrications of memristor devices with excellent performance.

Keywords: titanium oxide memristor, simulation program with integrated circuit emphasis, dopant drift, tunnel barrier

PACS: 84.32.–y, 85.35.–p, 61.46.–w, 85.40.Bh **DOI:** 10.1088/1674-1056/23/6/068401

1. Introduction

Since the first physical realization[1] of the fourth basic circuit element — memristor,[2] titanium oxide memristor devices have received significant attention and been widely studied for modeling and design in the solid state device society. Recent research has already demonstrated its great potential in many circuit application fields, such as resistive random access memory,[3] chaotic circuit analysis,[4,5] digital logical operation,[6] etc. Currently, research mainly focuses on conductive properties, modeling, and applications. Bao *et al.*[7] investigated voltage–current relationships (VCRs) between two parallel memristive circuits and proved that the VCR between these two parallel memristive circuits is closely related to the circuit parameters, and the frequency and amplitude of the sinusoidal voltage stimulus. Li *et al*[8] built a simplified model to study the effects of pristine state on the forming process of conductive percolation channel with the increase of applied voltage. Tian and Xu[9] proposed a method for continuous memristance programming and utilized it in a first-order active filter as an example to show its applications in programmable filters. Fang *et al.*[10] proposed the simulation program with integrated circuit emphasis (SPICE) modeling of flux-controlled unipolar memristive devices based on the memristance versus state map and simulated the model in HSPICE using model parameters abstracted from real devices.

For materials with resistive switching, choosing different kinds of electrodes and using different materials with different doped materials lead to different conductive mechanisms, such as boundary drift, filament conduction, ion migration, Schottky barrier model, trap charging and discharging, space-charge-limited conduction, etc.[11] As a kind of resistive switching, titanium oxide memristor exhibits complex and changeable conductive behaviors, which have already been proved by physical experiments:[12,13] one possible reason is that several different mechanisms may coexist and different mechanisms could be dominant in different materials systems.[14] Strukov *et al.*[1] found that memristance arises naturally in nanoscale systems in which solid-state electronic and ionic transport are coupled under an external bias voltage. They also used dopant drift theory to describe the nonvolatile memories of memristors. Pickett *et al.*[15] utilized the Simmons *I*–*V* expression for a rectangular barrier to quantitatively describe the static transport and switching dynamics of a memristor, then used a tunnel barrier and a resistor which are connected in series to model the conductive process of the memristive device. Tian *et al.*[16] proposed a compatible circuit model to discuss and prove the possibility of the coexistence of dopant drift and a tunnel barrier in a memristor.

Zhou and Huang[17] used SPICE as the tool to simulate

*Project supported by the National Natural Science Foundation of China (Grant No. 61171017).

†Corresponding author. E-mail: txiaobo1985@gmail.com

© 2014 Chinese Physical Society and IOP Publishing Ltd

the theoretical model of memristors and changed the parameters in the model to see the influence of each parameter on the characteristics. Prodromakis *et al.*[18] found through experimental evidence that micro-meter-size memristors are viable with practical $R_{\rm OFF}/R_{\rm ON}$ ratios, but the change of cross section area results in the change of memristor conductive characteristics. Yang *et al.*[13] gave the details of oxygen gas and vacancies formation in the electroforming process of a memristive device, and their experimental V–I curves also exhibit the differences between memristor devices with different parameters or outer biases.

It is concluded from the above-mentioned research findings that parameters have close relations with conductive properties of memristors. Therefore, the change of parameters should be one of the main reasons for the change of characteristics and may provide some explanations for the complexity of memristor conduction. A kind of complex and undesired phenomenon exists in many published experimental results, such as the data shown in Fig. 1(c) in Ref. [12] and Fig. 1(b) in Ref. [13], V–I curves of memristors within several identical outer bias cycles do not coincide with each other. Such an instability precludes the understanding of the conductive processes of the memristor devices, while the design and practical applications need memristor devices with stable performances. Therefore, how to eliminate or reduce the undesired features and fabricate memristor devices for practical applications needs to be explored. The possibility of the coexistence of dopant drift and tunnel barrier conduction in a memristor, which was studied in Ref. [16], provides basic explanations for the undesired characteristics. However, there has been no detailed research about the influence of parameter change on the conductive characteristics in such a case.

In this paper, parameters which affect memristor conductions are divided into two groups. The first group relates to dopant drift and includes the average ion mobility, cross section area, initial-doped layer width, etc. The second one relates to tunnel barrier conduction and includes channel area, initial tunnel barrier width, barrier height, etc. The influences of parameters in each group are studied and simulated in SPICE in the corresponding case and then the influences of all parameters in the coexistence case are simulated. Compared with published experimental results, the influences of parameter change on conductive characteristics are studied and the complexity of memristor conduction are further explained in this paper. Moreover, theoretical methods of eliminating or reducing the coexistence of the two mechanisms are proposed in order to guide the fabrications of memristors with practicability.

The rest of this paper is organized as follows. Section 2 includes the detailed analyses of single existence and coexistence of dopant drift and tunnel barrier-based mechanisms in a memristor. Section 3 studies relations between parameters and physical variables which affect characteristics of memristors. Section 4 gives the simulation results and discusses the influences of parameter change on memristor properties. Section 5 discusses and proposes the methods of eliminating or reducing the unstable properties of memristors. Section 6 concludes the paper.

2. Conductive mechanism of titanium oxide memristor

Resistor, inductor, and capacitor are three traditional fundamental circuit elements. Charge $q(t)$, current $i(t)$, voltage $v(t)$, and magnetic flux $\varphi(t)$ are four electrical basic quantities. Theoretically, there should be six relations among the four electrical basic quantities. Two of them are defined through time t : $i = {\rm d}q/{\rm d}t$ and $v = {\rm d}\varphi/{\rm d}t$, the other three are defined through the definitions of fundamental circuit elements: $R = {\rm d}v/{\rm d}i$, $C = {\rm d}q/{\rm d}v$, and $L = {\rm d}\varphi/{\rm d}i$, only the relation between $q(t)$ and $\varphi(t)$ is missing. In 1971, Chua[2] hypothesized that a new basic circuit element must exist and called it a memristor.

Theoretically, the memristor could remember its history in terms of the transient resistance. The relationship between the two quantities $q(t)$ and $\varphi(t)$ is described below. Equations (1) and (2) describe the charge-controlled and flux-controlled memristors, respectively:

$$\varphi(t) = f(q(t)), \tag{1}$$

$$q(t) = f(\varphi(t)). \tag{2}$$

Take the charge-controlled memristor for example, the differential form of Eq. (1) is

$$\frac{{\rm d}\varphi}{{\rm d}t} = \frac{{\rm d}f(q)}{{\rm d}q}\frac{{\rm d}q}{{\rm d}t}. \tag{3}$$

According to the definitions of $\varphi(t)$ and $q(t)$, equation (3) could be transformed into

$$v(t) = \frac{{\rm d}f(q)}{{\rm d}q}i(t). \tag{4}$$

Theoretically, $q(t)$ records the device history of a memristor, since $q(t)$ is the time integration of $i(t)$. The value of transient resistance depends on the charge according to Eq. (4), so a theoretical memristor has a memorizing ability. The analysis for a flux-controlled memristor is similar.

The conductions based respectively on dopant drift and tunnel barrier are distinctly different from each other. The former occurs in the inner part of titanium oxide and has a certain

relation with formation and transfer of oxygen vacancies. The latter occurs at the interface between titanium oxide and electrodes, so it is associated with the formation of a tunnel barrier. However, the memristor with coexistence of dopant drift and a tunnel barrier exhibits changeable V–I features, which are closer to published physical experimental phenomena than the case of single dopant or tunnel barrier conduction.[16]

2.1. Dopant drift-based conductive mechanism

In practical applications, the structure and equivalent circuit of a typical titanium oxide memristor which is fabricated by photolithography then followed by evaporation and lift-off,[19] are shown in Fig. 1(a). There are mainly four parts as follows. Top and bottom electrodes are made of platinum, the undoped layer consists of stoichiometric titanium oxide with an oxygen-to-titanium ratio of 2–1,[20] thus there are hardly any chances for oxygen atoms to move randomly, which leads to relatively poor conductivity. The doped layer consists of titanium oxide with oxygen vacancies and an oxygen-to-titanium ratio from $2-x$ to 1. Such a ratio indicates that oxygen element is deficient compared with in the undoped layer, so the doped layer has better conductivity, which is because there are charged oxygen vacancies that act as dopants and could move randomly inside. The part in which there is no electrode is the so-called active region and the widths of doped and undoped layers are $w(t)$ and $D-w(t)$, respectively. Each titanium oxide layer shares the same square cross section and area $S_{\rm to}$ equals a^2.

According to the theory of dopant drift,[21] the active region is equivalent to two variable resistors which are connected in series and the change rate of w with time t is proportional to titanium oxide current $i_{\rm to}(t)$.

$$R_{\rm M} = \frac{w}{D}R_{\rm ON} + \left(1-\frac{w}{D}\right)R_{\rm OFF}, \tag{5}$$

$$\frac{{\rm d}w(t)}{{\rm d}t} = F(w)\mu_{\rm v}\frac{R_{\rm ON}}{D}i_{\rm to}(t), \tag{6}$$

where $R_{\rm M}$ is the transient resistance of the active region, and equals $R_{\rm ON}$ and $R_{\rm OFF}$ in the cases of $w=D$ and $w=0$ respectively; μ_v is the average ion mobility; $F(w)$ is the window function which is adopted to compensate for differences between experimental measurements and the memristor model due to nonlinear dopant drift and boundary effects. In the case of linear dopant drift, $F(w)=1$.

2.2. Tunnel barrier-based conductive mechanism

Pickett *et al.*[15] first utilized sputter deposition to fabricate a Pt/TiO_2/Pt structure, and then used an electroforming process to realize a titanium oxide memristive device inside the structure. It was found that one of the interfaces between platinum electrodes and titanium oxide is ohmic contact, but the other exhibits electron tunnel barrier characteristics: such an asymmetry result in asymmetric V–I characteristics of the device. As shown in Fig. 1(b), after electroforming, a tunnel barrier with a width of δ is formed under the top electrode, meanwhile, part of the undoped titanium oxide is changed into a conductive channel which consists of doped titanium oxide and it exhibits great conductivity. Based on the above-mentioned findings, a tunnel barrier and a resistor are connected in series to model the conductive process of the memristor.

According to the theory of Simmons tunneling model of a rectangular barrier with image force,[21] the tunnel barrier current $i_{\rm tb}(t)$ satisfies[15]

$$i_{\rm tb} = \frac{j_0 A}{\Delta\delta^2}\{\phi_{\rm I}{\rm e}^{-B\sqrt{\phi_{\rm I}}} - (\phi_{\rm I}+e|v_{\rm g}|{\rm e}^{-B\sqrt{\phi_{\rm I}+e|v_{\rm g}|}})\}, \tag{7}$$

$$v_{\rm g} = v_{\rm active}(t) - i_{\rm tb}R_{\rm S}, \tag{8}$$

where A is the channel area, $v_{\rm g}$ is the voltage across the tunnel barrier, $v_{\rm active}(t)$ is the voltage across the active region of the device, e is the electron charge, and other parameters, such as B, λ, j_0, δ_1, δ_2, $\Delta\delta$, and Φ_1 are demonstrated in the supplementary material of Ref. [15].

The change rate of δ varying with t strongly depends on the magnitude and polarity of tunnel barrier current. In the cases of $i_{\rm tb}>0$ and $i_{\rm tb}<0$, its values are given by Eqs. (3) and (4) in Ref. [15], respectively.

2.3. Coexistence of dopant drift and a tunnel barrier

According to the discussion about the possibility of the coexistence of dopant drift and a tunnel barrier in a memristor,[16] the tunnel barrier and its series-connected conductive channel are regarded as part I. Theoretically, they share the same electrodes under the identical outer voltage bias with the rest of titanium oxide, which is regarded as part II as shown in Fig. 1(c). Though part II mainly consists of undoped titanium oxide, it is a mixture of doped and undoped titanium oxide with an ultra-low value of initial-doped layer width w_0. The ratio of oxygen to titanium ranges from 2.00 ± 0.01 to 1, which is observed by x-ray diffraction (XRD), transmission electron microscopy (TEM), and Rutherford backscattering spectrometry (RBS) analyses,[15] proving that a few oxygen vacancies or ions exist and act as dopants inside the titanium oxide. Therefore, it is reasonable that parts I and II are connected in parallel.[16]

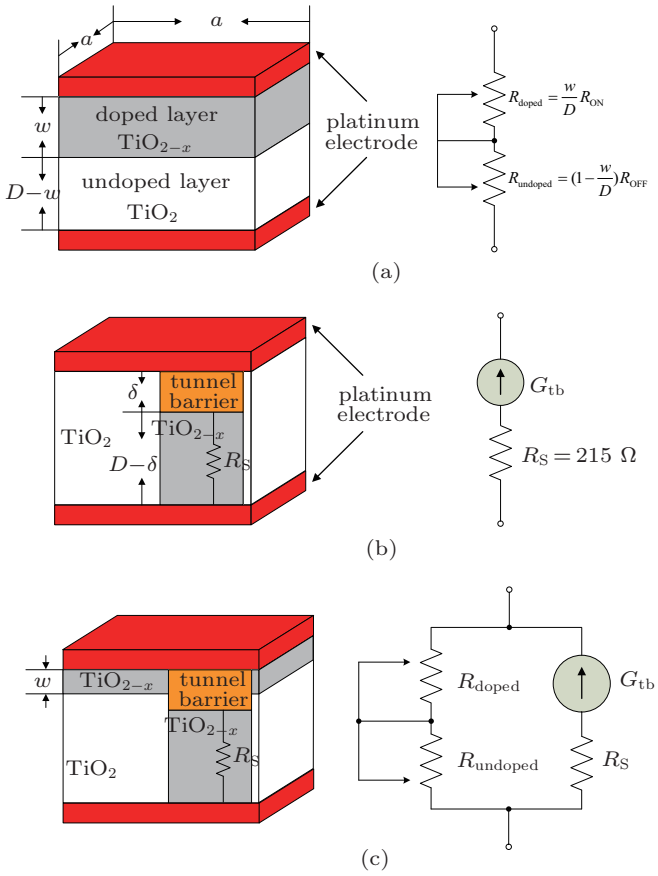


Fig. 1. (color online) Typical structures and equivalent circuits of memristors, which are fabricated (a) by photolithography followed by evaporation and lift-off and (b) by electroforming respectively. Panel (c) shows the memristor with coexistence of dopant drift and a tunnel barrier.

According to Ohm's law, in the case of coexistence of dopant drift and a tunnel barrier in a memristor, we have

$$v(t) = v_{\text{active}}(t) + i_{\text{mem}} R_{\text{E}}, \tag{9}$$

$$i_{\text{to}} = \frac{v_{\text{active}}}{R_{\text{to}}}, \tag{10}$$

$$i_{\text{tb}} = \frac{v_{\text{active}}}{R_{\text{tb}} + R_{\text{S}}}, \tag{11}$$

$$i_{\text{mem}} = i_{\text{to}} + i_{\text{tb}}, \tag{12}$$

$$R_{\text{M}} = \frac{v_{\text{active}}}{i_{\text{mem}}}, \tag{13}$$

where R_{to} and R_{tb} are the transient resistances of part II and the tunnel barrier, respectively, $v(t)$ is the outer voltage bias, R_{E} is the resistance of the electrode, i_{to} is the current of the titanium oxide which includes part II, and i_{mem} is the current of the memristor.

3. Analyses of relations between parameters and physical variables of the memristor

Parameters are closely related to conductive properties of memristor, which has been proved by many experimental and simulation studies. In this section, parameters are divided into two groups, which relate to dopant drift and tunnel barrier conduction, respectively. Each group of parameters is analyzed in the corresponding case. The outer bias and window function are not memristor's own parameters, however, both of them affect conductive characteristics of the device and could be considered as its own parameters.

The resistance R of a given material depends on length l, average cross-sectional area s, and its electrical resistivity ρ, and they are related by

$$R = \rho \frac{l}{s}. \tag{14}$$

Therefore, the case of single dopant drift exists in a memristor. The doped and undoped titanium oxide could be regarded as two kinds of materials which are connected in series. R_{ON} and R_{OFF} depend on their electrical resistivities respectively when the structure of the memristor is fixed, and they are expressed as follows:

$$R_{\text{ON}} = \rho_{\text{doped}} \frac{D}{S_{\text{to}}}, \tag{15}$$

$$R_{\text{OFF}} = \rho_{\text{undoped}} \frac{D}{S_{\text{to}}}, \tag{16}$$

where ρ_{doped} and ρ_{undoped} are the electrical resistivities of the doped and undoped titanium oxide, respectively, ρ_{undoped} is fixed, since there are no dopants in the undoped area of the device. However, ρ_{doped} varies with dopant density in the doped area. Suppose that the ratio between ρ_{undoped} and ρ_{doped} is k_{to}

$$k_{\text{to}} = \frac{\rho_{\text{undoped}}}{\rho_{\text{doped}}}. \tag{17}$$

Therefore, $R_{\text{OFF}} = k_{\text{to}} R_{\text{ON}}$. According to the mathematical definition, the value of doped layer width depends on its initial value w_0 and the change rate of w varying with t, so the transient resistance of the memristor depends on parameters which include $F(w)$, $v(t)$, μ_v, S_{to}, w_0, k_{to}, and D. The change rate of w with t depends on parameters which include $F(w)$, μ_v, w_0, k_{to}, D, and $v(t)$, since

$$\begin{aligned} R_{\text{M}} &= \frac{w}{D} R_{\text{ON}} + \left(1 - \frac{w}{D}\right) R_{\text{OFF}} \\ &= \frac{\rho_{\text{undoped}}}{S_{\text{to}}} \left(\frac{w}{k_{\text{to}}} + (D - w)\right), \end{aligned} \tag{18}$$

$$\begin{aligned} \frac{\mathrm{d}w(t)}{\mathrm{d}t} &= F(w)\mu_{\text{v}} \frac{R_{\text{ON}}}{D} i_{\text{to}}(t) \\ &= F(w)\mu_{\text{v}} \frac{v_{\text{active}}(t)}{(w + k_{\text{to}}(D - w))}, \end{aligned} \tag{19}$$

$$v_{\text{active}}(t) = v(t) - i_{\text{to}}(t) R_{\text{E}}. \tag{20}$$

The case of single tunnel barrier conduction exists in a memristor, according to Eq. (S1) and Eq. (S2) in the supplementary material of Ref. [15], both the change rate of δ varying with t and the tunnel barrier current depend on parameters which include A, δ_0, Φ_0, and $v(t)$, where δ_0 and Φ_0 are the initial barrier width and barrier height, respectively.

Table 1. Relations between parameters and physical variables of memristors.

Memristor parameters	Affected physical variables (in the case of dopant drift)	Affected physical variables (in the case of tunnel barrier conduction)
μ_v, w_0, k_{to}, D, $F(w)$	R_M and dw/dt	
S_{to}	R_M	
$v(t)$	R_M and dw/dt	i_{tb} and $d\delta/dt$
A, δ_0, Φ_0		i_{tb} and $d\delta/dt$

In Table 1 are the above-mentioned analyses and the relations between parameters and physical variables which affect the conductions of memristors. Parameters which affect the tunnel barrier current must have an influence on the transient resistance of the tunnel barrier, since

$$v(t) = i_{tb}(t)(R_E + R_{tb} + R_S). \tag{21}$$

4. Simulation results

For studying the influences of parameters on the conductive characteristics of memristors, we take the control variate method to perform simulations in SPICE, which means only one parameter changes and others remain default values for each simulation. Our software is PSPICE 10.5, which is a widely used version. The model used in the simulation is a compatible circuit model which was proposed in Ref. [16]. The circuit which is adopted here for the simulation is shown in Fig. 2.

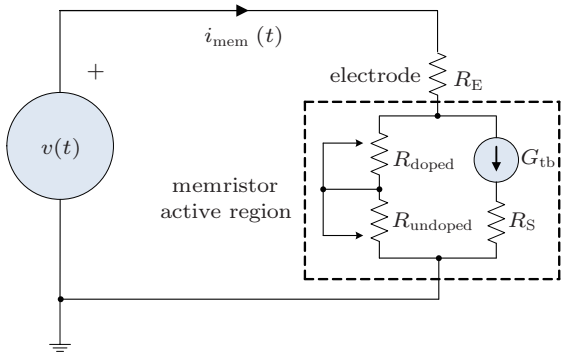


Fig. 2. Circuit structure for the simulation.

In the case of single existence of dopant drift, $\mu_v = 10^{-14}$ m^2·V^{-1}·S^{-1}, $D = 10$ nm, and $w_0 = 1$ nm.[16] Suppose that $R_{ON} = 200\ \Omega$ and $R_{OFF} = 10$ kΩ when $S_{to} = 25\ \mu$m^2, so $\rho_{doped} = 0.5\ \Omega$·m, $\rho_{undoped} = 25\ \Omega$·m, and $k_{to} = 50$. The resistances of two electrodes are negligible. $v(t) = v_0 \sin(2\pi f t)$, with $v_0 = 4.0$ V and $f = 1.0$ Hz. Simulation time span $T = 3/f$ and time step $\Delta t = 0.1$ ms. $vntol = 10^{-7}$ and $abstol = 1$ are the absolute voltage and current tolerance, respectively. $F(w/D) = 1 - [(w/D - 0.5)^2 + 0.75]^P$ is proposed in Ref. [22] and adopted as the window function in the simulation with $P = 1$. R_S is set to be an ultra-large value for eliminating the effect of the tunnel barrier conduction.

Figure 3(a) proves that μ_v is a variable which could affect dw/dt and R_M, since some external factors, such as temperature and radiation could change the ion mobility and result in the increase or decrease of dopant activeness, which have already been proved in Refs. [23] and [24]. Figures 3(c)–3(h) demonstrate that the increase of w_0, P, v_0 and decrease of k_{to}, D, f will enlarge the value of dw/dt and the variation range of R_M, which is consistent with Eqs. (18) and (19), since more dopants at the initial time result in a stronger initial current in the device, the decrease of k_{to} leads to the increase of ρ_{doped} and shortens the conduction difference between doped and undoped layers. The similar simulations of w_0 and k_{to} are discussed in Ref. [25]. Moreover, the increase of the outer bias amplitude and the decrease of the active region width lead to a stronger electric field inside the device. By comparing with the study of influences on memristor V–I curves caused by the change of v_0 in Ref. [26], figure 3(g) proves that the change of dw/dt is the direct result caused by the change of v_0 which then leads to a difference in device current.

As shown in Figs. 3(f) and 3(h), a larger amplitude of the window function corresponds to a larger value of dw/dt and variation range of R_M, which is consistent with Fig. 7 in Ref. [22]. Dopant drift is sensitive to the frequency of $v(t)$, since the outer bias with a smaller frequency has a larger period and results in more charges which flow through the active region of the device, thus the variation range of R_M increases. Similar simulation results are also given in Fig. 3 in Ref. [27].

Figure 3(b) proves that the change of S_{to} is independent of dw/dt, which is consistent with Eq. (19). It could be concluded that a memristor with a large cross section area equals several memristors which are connected in parallel in the same direction and have the same cross section area, but the increase of S_{to} leads to a decrease of the variation range of R_M, which is consistent with Fig. 6 in Ref. [27], since the increase of cross section area results in the decrease of the resistance of a given material.

In the case of single existence of tunnel barrier, $A = 10^4$ nm^2, $\Phi_0 = 0.95$ eV, $e^2\ln(2)/(8K\varepsilon_0) = 0.0998$, $\delta_1 = 0.1261$ nm, $f_{off} = 3.5\ \mu$s, $i_{off} = 115\ \mu$A, $a_{off} = 1.2$ nm, $f_{on} = 40\ \mu$s, $i_{on} = 8.9\ \mu$A, $a_{on} = 1.8$ nm, $b = 500\ \mu$A, $\delta_c = 0.107$ nm, $\delta_0 = 1.1$ nm, $R_S = 215\ \Omega$, and $R_E = 2.4$ kΩ.[28] $v(t)$ is a triangular wave with a period of $T_{tri} = 6$ s which is shown in the inset of Fig. 4(a). The maximal and minimal values of $v(t)$ are $v_{max}(t) = 6.0$ V and $v_{min}(t) = -3.0$ V, respectively. $T = T_{tri}$ and $\Delta t = 0.1$ ms. $vntol = 10^{-8}$. R_{doped} and $R_{undoped}$ are set to be ultra-large values for eliminating the effect of the dopant drift. Others remain the same.

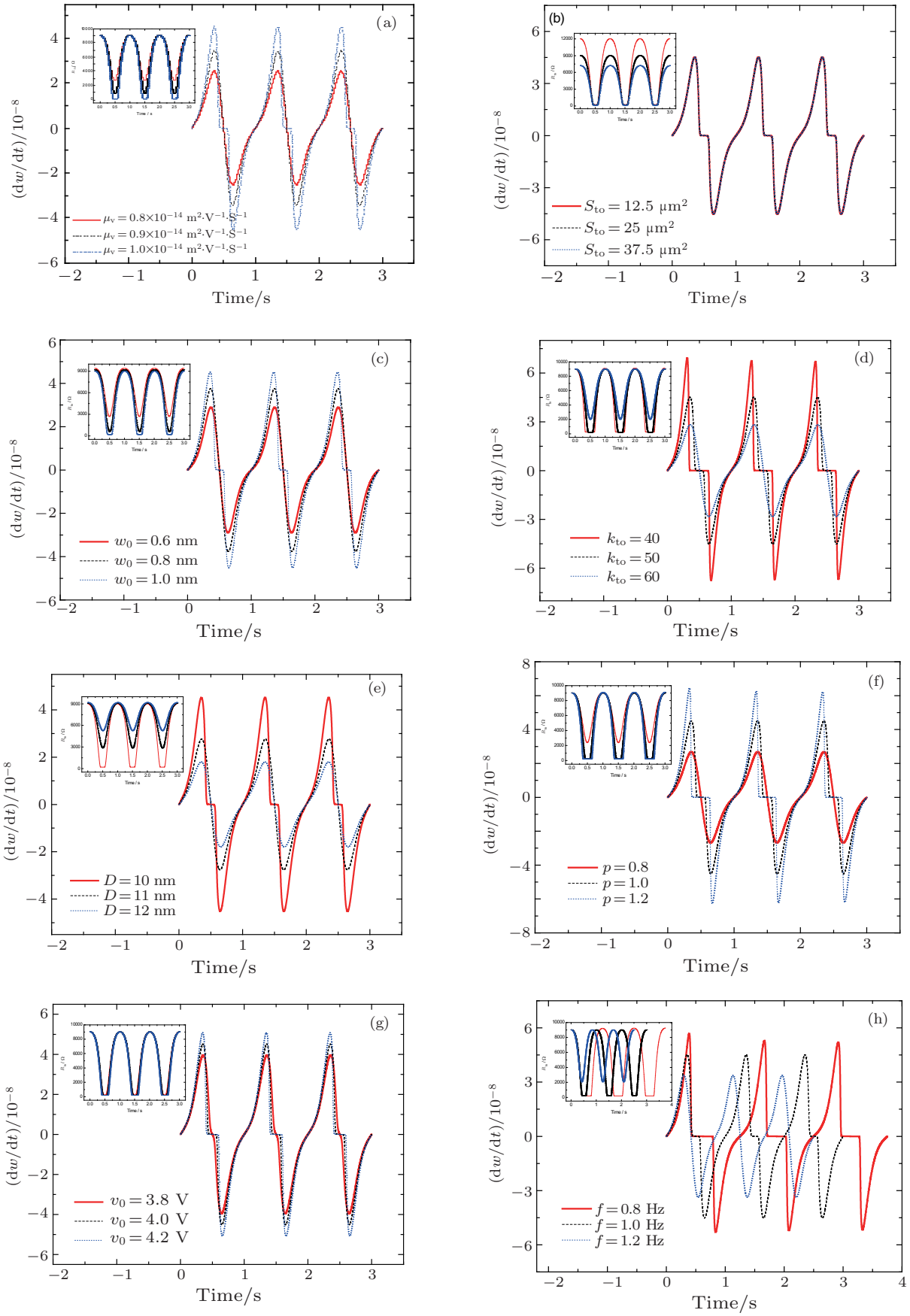


Fig. 3. (color online) Influences of parameter change on dw/dt and R_{to} in the case of existence of single dopant drift, with (a) $\mu_v = 8\times10^{-15}$, 9×10^{-15}, 1×10^{-14} m^2·V^{-1}·S^{-1}; (b) $S_{to} = 12.5$, 25, 37.5 μm^2; (c) $w_0 = 0.6$, 0.8, 1.0 nm; (d) $k_{to} = 40$, 50, 60; (e) $D = 10$, 11, 12 nm; (f) $P = 0.8$, 1.0, 1.2; (g) $v_0 = 3.8$, 4.0, 4.2 V; (h) $f = 0.8$, 1.0, 1.2 Hz. The inset in each panel shows the change of R_{to} with time in the corresponding case.

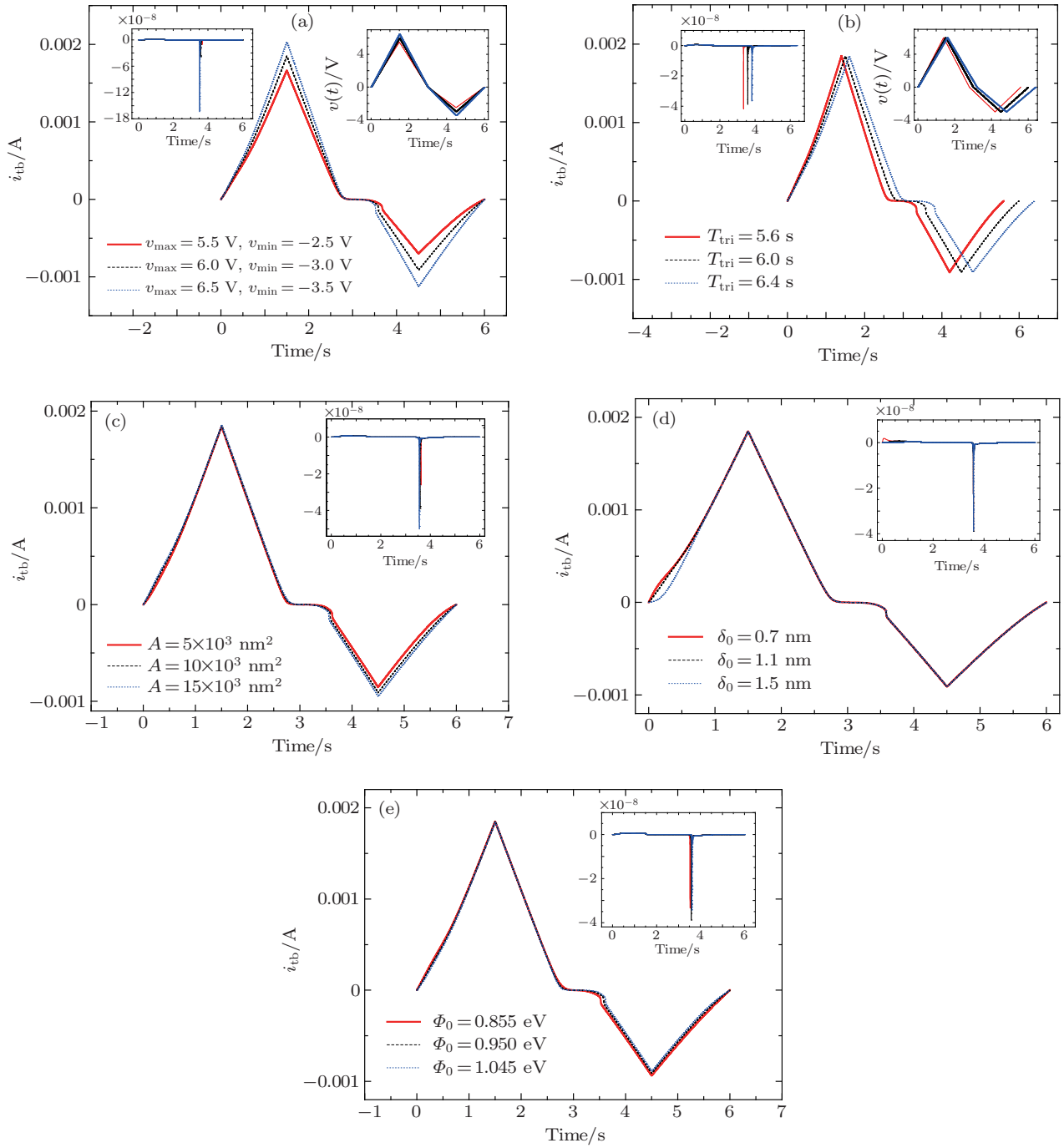


Fig. 4. (color online) Influences of parameter change on i_{tb} and $d\delta/dt$ in the case of existence of single tunnel barrier, with (a) $v_{max}(t) = 5.5$ V, $v_{min}(t) = -2.5$ V; $v_{max}(t) = 6.0$ V, $v_{min}(t) = -3.0$ V; $v_{max}(t) = 6.5$ V, and $v_{min}(t) = -3.5$ V; (b) $T_{tri} = 5.6$, 6.0, 6.4 s. The left and right insets show the changes of $d\delta/dt$ and the outer bias $v(t)$, respectively; (c) $A = 5\times10^3$, 10^4, 1.5×10^4 nm^2; (d) $\delta_0 = 0.7$, 1.1, 1.5 nm; (e) $\Phi_0 = 0.855$, 0.950, 1.045 eV. The inserts in panels (c), (d), and (e) show the changes of $d\delta/dt$ with time.

According to Eqs. (7) and (8) in the present paper and Eqs. (3) and (4) in Ref. [15], larger amplitude of outer bias $v(t)$ results in the increase of the voltage across the active region, thus enlarging the current in the tunnel barrier and the $d\delta/dt$ as well, which is shown in Fig. 4(a). Similar results are given in Fig. 3 in Ref. [15]. Figure 4(b) proves that the tunnel barrier conduction is sensitive to the frequency of the outer bias. Though the amplitude of i_{tb} does not obviously change, the peak value of $d\delta/dt$ decreases as T_{tri} increases. The variation ranges of channel area and barrier height are $10^4 \pm 2.5\times10^3$ nm^2 and 0.95 ± 0.03 eV.[16] However, there has been no further analysis on the effects of the two parameters which vary in their own ranges. According to Eq. (7) in the present paper and Eqs. (3) and (4) in Ref. [15], the increase of channel area results in the increase of tunnel barrier current and change of $d\delta/dt$, which is proved by Fig. 4(c). Figure 4(d) proves that δ_0 relates to i_{tb} and $d\delta/dt$, but the influences of the change of δ_0 on i_{tb} and $d\delta/dt$ mainly con-

centrate in the initial period of time. Figure 4(e) proves that the change of Φ_0 has influences on $i_{\rm tb}$ and $\mathrm{d}\delta/\mathrm{d}t$, which is consistent with Eqs. (S1) and (S2) in the supplementary material of Ref. [15]. However, the relation between Φ_0 and $i_{\rm tb}$ is complicated and nonlinear. Moreover, the conducting channel formed through the electroforming process often has a wide variance of properties depending on how the electroforming process takes place. This variance of properties has relatively limited the applications of metal oxide switches in computing devices.[29] By comparing with Fig. 4, it is a reasonable explanation that parameter changes caused by the instability of the tunnel barrier formation lead to the changeable characteristics of the device.

In the case of coexistence of dopant drift and tunnel barrier conduction in a memristor, parameters adopted in the simulations are consistent with those utilized in Figs. 3 and 4 except that $w_0 = 1 \times 10^{-4}$ nm. Since there are few dopants in titanium oxide, $v(t)$ which is utilized in the simulations shown in Fig. 4 is adopted as the outer bias and its maximal and minimal values are $v_{\rm max}(t) = 6.0$ V and $v_{\rm min}(t) = -3.0$ V, respectively, with a period of 6 s. $R_{\rm E} = 2.4$ kΩ, $R_{\rm S} = 215$ Ω, $R_{\rm doped}$ and $R_{\rm undoped}$ are set according to Eq. (18). Simulation time span $T = 3T_{\rm tri}$ and time step $\Delta t = 0.1$ ms. Other parameters remain unchanged.

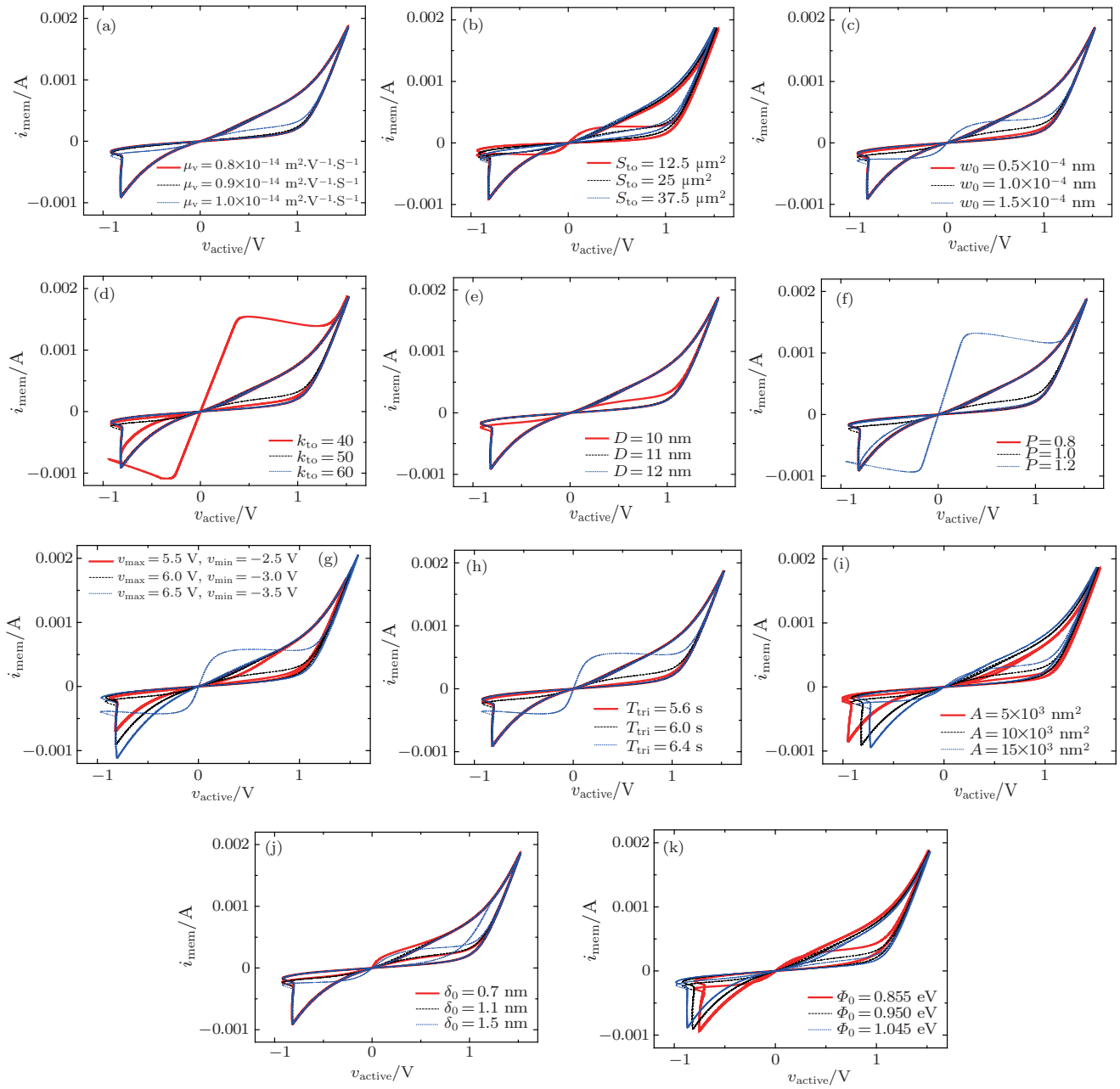


Fig. 5. (color online) Influences of parameter change on V–I characteristics in the case of coexistence of dopant drift and a tunnel barrier in a memristor, with (a) $\mu_{\rm v} = 8\times10^{-15}$, 9×10^{-15}, 1×10^{-14} m^2·V^{-1}·S^{-1}; (b) $S_{\rm to} = 12.5$, 25, 37.5 μm^2; (c) $w_0 = 0.6$, 0.8, 1.0 nm; (d) $k_{\rm to} = 40$, 50, 60; (e) $D = 10$, 11, 12 nm; (f) $P = 0.8$, 1.0, 1.2; (g) $v_{\rm max}(t) = 5.5$ V, $v_{\rm min}(t) = -2.5$ V; $v_{\rm max}(t) = 6.0$ V, $v_{\rm min}(t) = -3.0$ V; $v_{\rm max}(t) = 6.5$ V, $v_{\rm min}(t) = -3.5$ V; (h) $T_{\rm tri} = 5.6$, 6.0, 6.4 s; (i) $A = 5\times10^3$, 1.0×10^4, 1.5×10^4 nm^2 ; (j) $\delta_0 = 0.7$, 1.1, 1.5 nm; (k) $\Phi_0 = 0.855$, 0.950, 1.045 eV.

The changes of different parameters cause different influences on the device conduction as shown in Figs. 5(a)–5(h), the increase of μ_v, w_0, P, v_0, T_{tri} and decrease of S_{to}, k_{to}, D strengthen the influence of the dopant drift on the device conduction, even letting dopant drift play a major role as shown in Figs. 5(d) and 5(f). The increase of the amplitude of $v(t)$ results in the increase of $i_{mem}(t)$ as shown in Fig. 5(g), and the increase of A and decrease of Φ_0 lead to the decrease of the peak value of $v_{active}(t)$ when $v_{active}(t) < 0$ as shown in Figs. 5(i)–5(k). The influence of δ_0 on V–I characteristics of memristor is not so obvious as shown in Fig. 5(j), since the influences of the change of δ_0 on i_{tb} and $\mathrm{d}\delta/\mathrm{d}t$ mainly concentrate in the initial period of time, which has already been proved by Fig. 4(d).

5. Discussion about eliminating the coexistence

The conductive characteristics of a memristor with the coexistence of dopant drift and tunnel barrier exhibit complexity which is different from those of single dopant drift or single tunnel barrier conduction, since in such a case, the conduction of the device is a mixture of two different mechanisms. The titanium oxide which contains dopants shows changeable features compared with the stable V–I characteristics of tunnel barrier conduction, since the asymmetric outer bias results in an increment of the initial doped layer width in each voltage cycle, when the changeable conduction of dopant drift adds to the stable conduction of the tunnel barrier, then the V–I characteristics of the device become unstable. Compared with the coexistence case discussed in Ref. [16], changes of parameters which relate to dopant drift or tunnel barrier result in the change of the transient resistance and voltage of the active region, which in turn affects the conduction of dopant drift or tunnel barrier and intensifies the conductive complexity. However, no matter which parameter changes, the changeable property of V–I curve exists, which is closer to physical experimental phenomena published in Refs. [12], [13], [30], and [31] than in the case of single dopant drift or tunnel barrier conduction.

The changeable features of memristors are undesired, since the design and applications of memristors need devices with stable performances. For eliminating the changeable features, theoretically the coexistence of dopant drift and tunnel barrier needs to be broken. A controlled addition of dopants in memristor active regions proposed in Ref. [32] allows the reconfiguration of the active region. Approaches proposed in Ref. [33] improves the switching performance of the filament-type RRAM by doping, process optimization and interface engineering. Compared with the above-mentioned methods, our suggestions are rather simple and easy to realize. The first suggestion is to select pure stoichiometric titanium oxide without dopants as the material of the device, since initial dopants in the titanium oxide cause instability, which is proved in simulations shown in Fig. 5. The second one is to fabricate the device layer by layer instead of electroforming and keep only dopant drift in the device, since the formation process and parameter stability of the tunnel barrier are more difficult to control than the doped layer, which has already been demonstrated in Ref. [34].

If the existence of dopants in titanium oxide is inevitable, it is better to increase the width of the active region and the cross section area, thereby narrowing the variation range of the transient resistance of titanium oxide. Furthermore, reducing the amplitude and increasing the frequency of the outer bias could also weaken the effect of dopant drift. The average ion mobility and the ratio between $\rho_{undoped}$ and ρ_{doped} relate to temperature and material type, respectively, then we can control the activity of dopants and the resistivity of the doped layer by controlling the ambient temperature and selecting suitable material with small value of μ_v and large value of k_{to} to lower the influence of dopant drift. However, in such a case, it is an urgent need to prove the effectiveness of the theoretical methods by physical experimental tests.

6. Conclusions

Titanium oxide memristors exhibit complex conductive characteristics, for which one possible reason is that dopant drift and tunnel barrier conduction coexist and affect the conductive process of the device together. In this paper, in the cases of single existence and coexistence of dopant drift and tunnel barrier conduction, the relations between parameters and physical variables which affect conductions of a memristor are studied, and the influences of each parameter change are analyzed and simulated. It is found that parameter change has an effect on dopant drift and tunnel barrier conduction, and that the mutual influence of the two conductive processes intensifies the complexity of the device conduction, based on which, in this paper also presented are the principles and suggestions on how to eliminate or reduce the undesired changeable features and fabricate physical memristors with excellent performance. Experimental tests and quantitative study will be our future work.

References

[1] Strukov D B, Snider G S, Stewart D R and Williams R S 2008 *Nature* **453** 80
[2] Chua L O 1971 *IEEE Trans. Circ. Theory* **18** 507
[3] Fang X D, Tang Y H and Wu J J 2012 *Chin. Phys. B* **21** 098901
[4] Bao B C, Hu W, Xu J P, Liu Z and Zou L 2011 *Acta Phys. Sin.* **60** 120502 (in Chinese)
[5] Bao B C, Liu Z and Xu J P 2010 *Acta Phys. Sin.* **59** 3785 (in Chinese)
[6] Raja T and Mourad S 2009 *International Conference on Communications, Circuits and Systems*, July 23–25, 2009, Milpitas, California, USA, p. 939
[7] Bao B C, Feng F, Dong W and Pan S H 2013 *Chin. Phys. B* **22** 068401
[8] Li Z W, Liu H J and Xu X 2013 *Acta Phys. Sin.* **62** 096401 (in Chinese)

[9] Tian X B and Xu H 2013 *Chin. Phys. B* **22** 088501
[10] Fang X D, Tang Y H, Wu J J, Zhu X, Zhou J and Huang Da 2013 *Chin. Phys. B* **22** 078901
[11] Huang D, Wu J J and Tang Y H 2013 *Chin. Phys. B* **22** 038401
[12] Miao F, Strachan J P, Yang J J, Zhang M X, Goldfarb I, Torrezan A C, Eschbach P, Kelley R D, Ribeiro G M and Williams R S 2011 *Adv. Mater.* **23** 5633
[13] Yang J J, Miao F, Pickett M D, Ohlberg D A A, Stewart D R, Lau C N and Williams R S 2009 *Nanotechnology* **20** 215201
[14] Yang J J, Pickett M D, Li X M, Ohlberg D A A, Stewart D R and Williams R S 2008 *Nature Nanotechnology* **3** 429
[15] Pickett M D, Strukov D B, Borghetti J L, Yang J J, Snider G S, Stewart D R and Williams R S 2009 *J. Appl. Phys.* **106** 074508
[16] Tian X B, Xu H and Li Q J 2013 *Chin. Phys. B* **22** 088502
[17] Zhou J and Huang D 2012 *Chin. Phys. B* **21** 048401
[18] Prodromakis T, Michelakis K and Toumazou C 2010 *Electron. Lett.* **46** 63
[19] Prodromakis T, Michelakis K and Toumazou C 2010 *International Workshop on Cellular Nanoscale Networks and Their Applications*, February 3–5, 2010, Bberkeley, California, USA, p. 1
[20] Williams R S 2008 *Spectrum IEEE* **45** 28
[21] Simmons J 1963 *J. Appl. Phys.* **34** 1793
[22] Prodromakis T, Peh Boon Pin, Papavassiliou C and Toumazou C 2011 *IEEE Trans. Electron Dev.* **58** 3099
[23] Vujisic M, Stankovic K, Marjanovic N and Osmokrovic P 2010 *IEEE Trans. Nucl. Sci.* **57** 1798
[24] Mladenov V and Kirilov S 2013 *International Symposium on Theoretical Electrical Engineering*, June 24–26, 2013, Pilsen, Czech Republic, p. 6
[25] Zhang X, Zhou Y Z, Bi Q, Yang X H and Zu Y X 2010 *Acta Phys. Sin.* **59** 6673 (in Chinese)
[26] Yakopcic C, Taha T M, Subramanyam G, Pino R E and Rogers S 2011 *IEEE Electron Dev. Lett.* **32** 10
[27] Niu D M, Chen Y R, Xu C and Xie Y 2010 47*th ACM/IEEE Design Automation Conference*, June 13–18, 2010, Anaheim, USA, p. 877
[28] Abdalla H and Pickett M D *International Symposium on Circuits and Systems*, May 15–18, 2011, Rio de Janeiro, Brazil, p. 1832
[29] Zhang M X, Yang J H and Williams R S (US Patent) US2011/044734 [2013-01-24]
[30] Yoon K J, Lee M H, Kim G H, Song S J, Seok J Y, Han S, Yoon J H, Kim K M and Hwang C S 2012 *Nanotechnology* **23** 185202
[31] Yang J J, Strachan J P, Miao F, Zhang M X, Pickett M D, Yi W, Ohlberg D A A, Ribeiro G M and Williams R S 2011 *Appl. Phys. A* **102** 785
[32] Quitoriano N J, Kuekes P J and Yang J H (US Patent) US2011/0266510 A1 [2011-11-3]
[33] Lian W T, Long S B, Lu H B, Liu Q, Li Y T, Zhang S, Wang Y, Huo Z L, Dai Y H, Chen J N and Liu M 2011 *Chin. Sci. Bull.* **56** 461
[34] Strachan J P, Yang J J, Montoro L A, Ospina C A, Ramirez A J, Kilcoyne A L D, Ribeiro G M and Williams R S 2013 *Beilstein J. Nanotechnol.* **4** 467